Performance Evaluation of Si, SiC, and GaN Based Boost Converters for Photovoltaic Applications Using MPC-CNN Duty Cycle Optimization

Vo Thanh Ha [1], Nguyen Tan Phuc Lam [1], Tran Thuy Quynh [2], and Nguyen Hong Quang [3,*]
[1] Faculty of Electrical Engineering, University of Transport and Communications, Hanoi, Vietnam
[2] Faculty of Electrical and Electronic Engineering, University of Economics - Technology for Industries, Hanoi, Vietnam
[3] Faculty of Mechanical, Electrical, and Electronic Technology, Thai Nguyen University of Technology, Thai Nguyen, Vietnam
Email: votthanhha.ktd@utc.edu.vn (V.T.H.), lamnguyen24012008@gmail.com (N.T.P.L.), tranthuyquynh_uneti@gmail.com (T.T.Q.), quang.nguyenhong@tnut.edu.vn (N.H.Q.)

Manuscript received May 24, 2025; revised July 20, 2025; accepted August 2, 2025
*Corresponding author

***Abstract*—This paper presents a novel hybrid control strategy for DC-DC boost converters in Photovoltaic (PV) systems, combining Model Predictive Control (MPC) with Convolutional Neural Networks (CNN) to optimise the duty cycle in real time. The MPC–CNN framework leverages MPC's predictive accuracy and constraint-handling with CNN's fast inference and adaptability, ensuring robust voltage regulation under varying irradiance and load conditions. The hybrid scheme dynamically selects between CNN and MPC outputs based on real-time performance metrics, balancing response speed and control precision. Simulations with a 100-kW dynamic Photovoltaic (PV) profile demonstrate that MPC achieves near-zero steady-state error, while CNN provides faster transient responses. The hybrid controller surpasses both in maintaining voltage stability and energy efficiency. Additionally, a performance comparison of semiconductor technologies—Silicon (Si), Silicon Carbide (SiC), and Gallium Nitride (GaN)—shows that GaN-based converters achieve the best results, with 97.6% efficiency, 2.8 V ripple, 6.4 W switching loss, and the fastest transient response of 0.17 ms. These findings confirm the effectiveness of the CNN-enhanced MPC approach and establish GaN's superiority for compact, high-performance PV applications. Future work will explore real-time embedded implementation, adaptive CNN retraining, and integration into smart grid and energy management systems.**

***Index Terms*—Gallium Nitride (GaN), Model Predictive Control (MPC)-Convolutional Neural Networks (CNN), Photovoltaic (PV), Silicon (Si), Silicon Carbide (SiC)**

NOMENCLATURE

Abbreviation	Full Form
PV	Photovoltaic
MPC	Model Predictive Control
CNN	Convolutional Neural Network
Si	Silicon
SiC	Silicon Carbide
GaN	Gallium Nitride
DC-DC	Direct Current to Direct Current
PWM	Pulse Width Modulation
RMSE	Root Mean Square Error
MAE	Mean Absolute Error
R^2	Coefficient of Determination
EMI	Electromagnetic Interference
FLC	Fuzzy Logic Control
ANFIS	Adaptive Neuro-Fuzzy Inference System
PPO	Proximal Policy Optimization
WBG	Wide Bandgap
HIL	Hardware-in-the-Loop
VIN	Input Voltage
IIN	Input Current
VOUT	Output Voltage
IOUT	Output Current
G	Solar Irradiance
T	Temperature

I. INTRODUCTION

The growing global demand for renewable energy has increasingly emphasised the development of efficient, compact, and reliable power electronic converters, particularly for Photovoltaic (PV) systems. Among various DC-DC topologies, the boost converter remains a prevalent choice due to its ability to elevate low Photovoltaic (PV) voltages to levels suitable for grid-tied inverters or battery storage systems [1–5]. However, conventional Silicon (Si)–-based power devices are now facing physical and thermal performance limitations, such as low switching frequency, higher conduction losses, and inferior thermal dissipation, thereby hindering further improvement in power density and conversion efficiency [6, 7].

Wide Bandgap (WBG) semiconductors, especially Silicon Carbide (SiC) and Gallium Nitride (GaN), have emerged as superior alternatives to traditional Si due to their favourable electrical properties, including high breakdown voltage, fast switching speed, and better thermal conductivity [8–11]. SiC devices enable higher

doi: 10.18178/ijeetc.14.5.304-312

switching frequencies with reduced losses. At the same time, GaN transistors offer ultra-fast switching and reduced parasitic effects—making both materials attractive for high-efficiency solar power applications [12, 13].

Numerous studies have validated the performance superiority of SiC and GaN over Si. P. Zhang & Y. Yang *et al*. [14] laid the theoretical groundwork for SiC-based devices, while A. Udabe *et al*. [15] reported reduced switching losses with SiC in high-frequency operations. GaN's capability to minimise converter volume and electromagnetic interference (EMI) has been demonstrated by E. Zafra *et al*. [16], and its fast transient performance was highlighted by Di Maria *et al*. [17]. Moreover, F. Wang *et al*. [18] emphasised GaN's thermal robustness in dynamic PV environments. However, most of these contributions focus primarily on device-level or thermal characterisation, with limited work addressing intelligent control schemes for real-time optimisation under rapidly varying solar irradiance.

To address this gap, this paper proposes a hybrid control framework that dynamically integrates Model Predictive Control (MPC) and Convolutional Neural Networks (CNN) to optimise the duty cycle in boost converters [19]. The structure is depicted in Fig. 1. The control loop simultaneously evaluates the converter's output voltage $V_{out}(t)$ and current $I_{out}(t)$ through two channels: a physics-based MPC controller and a pre-trained CNN model. The MPC ensures mathematically rigorous prediction, while the CNN offers rapid inference for adaptive behaviour in real-time environments [20]. A hybrid logic selector chooses the most appropriate control signal based on performance criteria.

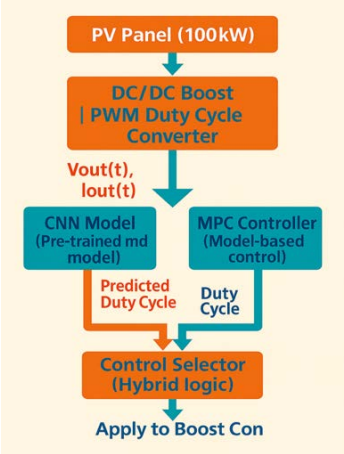

Fig. 1. The control structure of the intelligent energy management system for the boost DC/DC converter.

In recent years, numerous advanced control strategies have been proposed to enhance the dynamic performance and robustness of DC-DC boost converters, particularly in renewable energy applications with variable irradiance and load profiles. Traditional methods such as Fuzzy Logic Control (FLC) and Adaptive Neuro-Fuzzy Inference Systems (ANFIS) have shown effectiveness in handling system uncertainties and non-linearities, as demonstrated by Vo Thanh Ha [21] and Duranay *et al*. [22]. Meanwhile, adaptive sliding mode control techniques [23, 24] have improved transient response and voltage regulation, albeit with challenges in chattering and complexity tuning. More recently, reinforcement learning approaches, such as the Proximal Policy Optimization (PPO) framework proposed by Utsab Saha *et al*. [25], have emerged as model-free alternatives capable of learning optimal control policies from data.

On the other hand, the evolution of WBG devices such as GaN and SiC has opened new opportunities for high-frequency, high-efficiency converter designs, requiring intelligent control strategies that can leverage their full capabilities [26]. Hybrid model-based and learning-based control schemes are gaining increasing attention. Notably, the use of MPC in DC-DC converters allows for constraint-aware optimization and predictive stability [27, 28]. Furthermore, the integration of deep learning models such as CNNs has been explored to enhance real-time adaptability and generalization under dynamic operating conditions, as reported in the works by Sergio Lucia *et al*. [29], Li, Yuan *et al.* [30] and Sergio Lucia [31].

Building upon these advancements, the proposed study introduces a hybrid intelligent control framework that combines MPC with a pre-trained CNN to regulate the duty cycle in boost converters. While the MPC module ensures mathematical prediction and constraint handling, the CNN provides fast, data-driven inference to accommodate unpredictable environmental changes. A hybrid logic selector dynamically switches between control outputs based on predefined performance metrics, ensuring robust and efficient converter operation under real-time conditions. This integrated approach demonstrates improved performance over traditional controllers, particularly in terms of response time, ripple minimization, and adaptability to system disturbances.

The framework is validated through simulation across three semiconductor technologies—Si, SiC, and GaN—under a 100 kW dynamic PV profile. Key performance indicators (KPIs) are benchmarked, including output voltage ripple, energy efficiency, switching losses, and response time. This integrated approach not only highlights the synergistic potential of WBG materials with intelligent control strategies but also provides a scalable pathway towards high-performance, smart PV power conversion systems.

This study makes five major contributions:

- Comprehensive evaluation: A performance comparison of boost converters using Si, SiC, and GaN devices under real PV conditions.
- Hybrid MPC-CNN framework: A novel control structure integrating CNN for fast inference and MPC for optimal prediction.
- Real-time AI integration: The CNN-based duty prediction adapts to real-time PV profile changes to enhance energy capture.
- Simulation and Dataset: Python-based simulations using a benchmark dataset of over 4,000 PV operation samples.
- Material guidance: Results guide the practical

selection of semiconductor materials—GaN for compact, high-speed converters and SiC for high-power, thermally stressed environments.

Advancements in power semiconductor devices and intelligent control strategies have yet to close the research gap in real-time hybrid controllers that combine deep learning (e.g., CNN) with physics-based predictive control (e.g., MPC) for DC-DC converters under highly dynamic PV conditions. Current methods primarily depend on either model-based techniques or offline-trained networks, lacking the adaptability to sudden changes in solar irradiance or load demand. This paper addresses this issue by proposing a hybrid MPC-CNN control framework that dynamically balances rapid inference with optimal prediction, ensuring robust and efficient operation in real-world PV settings.

The paper is organised into five sections. Section I outlines the motivation, research gaps, and proposed solution. Section II introduces the boost converter model, PV panel characteristics, and the hybrid MPC-CNN control scheme. Section III explains the experimental setup, dataset preparation, and simulation configuration. Section IV presents and discusses the performance evaluation of all three material-control combinations using metrics such as RMSE, R^2, efficiency, and ripple. Finally, Section V summarises the findings, practical implications, and future directions—including hardware integration and smart energy platform deployment.

II. Modeling of Boost Converter and PV Load

A. Modeling of Boost Converter

Fig. 2 illustrates the schematic diagram of a boost DC/DC converter integrated with a Photovoltaic (PV) panel as its input source. The converter is composed of a DC input voltage source V_{in} (representing the PV panel), an inductor L, a switching unit formed by two MOSFETs M_1 andM_2, a diode (internal body diode of the MOSFET), an output capacitor C, and a load resistance R_{load}. When operated in switching mode, the converter steps up the input voltage to a higher output voltage U_{out} making it suitable for grid integration or battery charging in renewable energy systems. The two MOSFETs work in complementary switching to control the energy transfer from the inductor to the capacitor and load. The inductor stores energy when the switch is on and releases it when the switch is off, resulting in a boosted voltage across the output terminals. This topology is widely adopted in PV systems due to its simplicity, cost-effectiveness, and ability to maintain efficient energy conversion under varying solar irradiance and load conditions. The schematic serves as the foundation for further controller design, including the integration of CNN-based inference and MPC optimization strategies for real-time duty cycle control.

The dynamic behavior of the boost converter can be described by the averaged state-space equations:

$$\frac{dI_L(t)}{dt} = \frac{1}{L}\left[V_{\text{in}}(t) - \big(1 - D(t)\big)U_{\text{out}}(t)\right] \quad (1)$$

$$\frac{dU_{\text{out}}(t)}{dt} = \frac{1}{C}\left[\big(1 - D(t)\big)I_L(t) - \frac{U_{\text{out}}(t)}{R_{\text{load}}}\right] \quad (2)$$

where I_L is the inductor current, U_{out} is the output voltage, and $D(t)$ is the duty cycle in time domain.

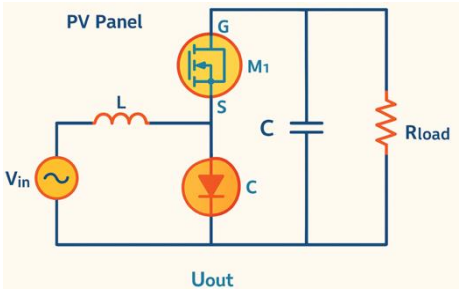

Fig. 2. The schematic diagram of a boost DC/DC converter integrated with a Photovoltaic (PV) panel.

B. Modeling of PV Load

Fig. 3 illustrates the single-diode equivalent circuit used to model the Photovoltaic (PV) panel. This model, widely adopted in PV system analysis, captures the nonlinear behavior of the solar cell by representing it with a current source in parallel with a diode, and optionally including series R_s and shunt R_{sh} resistances. The photocurrent source I_{phase} generates current proportional to solar irradiance, while the diode characterizes the p-n junction's response to voltage and temperature. The series resistance R_s accounts for internal losses due to current flow, and R_{sh} represents leakage paths within the cell. This model enables accurate prediction of the *I-V* and *P-V* characteristics under various environmental conditions, forming the foundation for control and optimization strategies in PV power conversion systems.

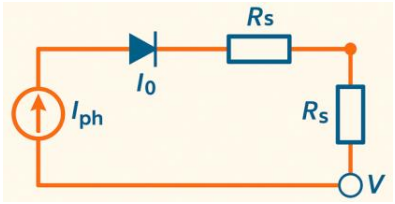

Fig. 3. Single-diode equivalent circuit.

The PV panel is modeled using a single-diode equivalent circuit, represented by:

$$I = I_{\text{phase}} - I_0\left(e^{\frac{V+IR_S}{nV_t}} - 1\right) - \frac{(U+IR_S)}{R_{\text{sh}}} \quad (3)$$

where I_{phase} is the photo current, I_S is the saturation current, R_s and R_{sh} are the series and shunt resistances, respectively. V is terminal voltage of the PV cell, n is diode ideality factor, V_t is thermal voltage, $V_t = kT/q$ with Boltzmann constant k, temperature T (K), and electron charge q.

III. MPC-CNN Based Duty Cycle Control

The CNN for duty cycle prediction uses four normalized inputs: input voltage V_{in}, input current I_{in}, solar irradiance G, and temperature T. Its architecture consists of three convolutional layers with ReLU activation, a flattening layer, and two fully connected layers, outputting

a continuous optimal duty cycle value. Trained with the Mean Squared Error (MSE) loss function for 50 epochs and a batch size of 128, the model is optimized for real-time inference on low-resource embedded devices like STM32 microcontrollers. Schematic diagram of an intelligent closed-loop control system for a DC-DC boost converter (Fig. 4), using two control strategies simultaneously:

- MPC: Control based on a mathematical model.
- CNN: Predictive control based on deep learning.

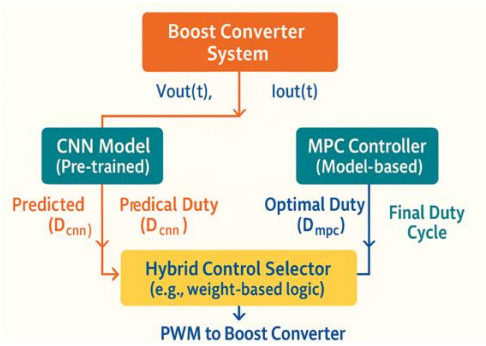

Fig. 4. A hybrid control strategy integrating MPC and CNN.

The proposed control framework integrates a CNN) and a MPC to optimize the Pulse-Width Modulation (PWM) duty cycle of a boost converter in Photovoltaic (PV) applications. The CNN is trained offline using MPC-generated datasets under varying irradiance and temperature conditions. Its input vector includes four normalized features: input voltage V_{in}, input current I_{in}, solar irradiance G, and temperature T. The architecture comprises three convolutional layers with ReLU activations, followed by a flattening layer and two fully connected layers. The output is a single continuous value representing the predicted duty cycle D. Training is performed using Mean Squared Error (MSE) loss over 50 epochs with a batch size of 128, ensuring generalization across dynamic PV profiles.

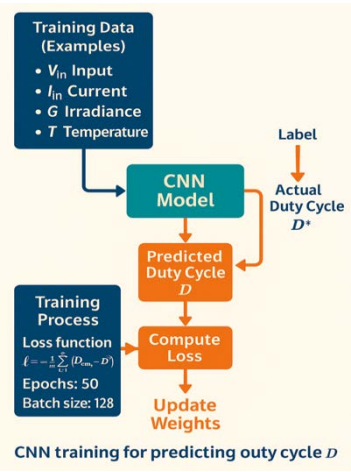

Fig. 5. The CNN training for predicting cycle D.

Once trained, the CNN provides low-latency approximations of the optimal duty cycle based on real-time measurements, while the MPC computes precise control actions using a discrete-time model over a prediction horizon. A hybrid selector receives outputs from both CNN and MPC and evaluates predefined criteria—such as voltage ripple, prediction error, or transient response. If system conditions remain stable and within threshold limits, the CNN output is selected for faster control. Otherwise, the selector switches to the MPC output for improved accuracy.

This hybrid approach combines the rapid inference capability of CNN with the precision of MPC, achieving high energy efficiency, robust voltage regulation, and adaptability to fluctuating environmental conditions. The overall control process is illustrated in Fig. 5.

MPC predicts the future states of the converter using a discrete-time model and computes the optimal duty cycle minimizing the cost function:

$$J = \sum_{k=1}^{N_p} (U_{\text{out}}(k) - U_{\text{ref}})^2 + \beta \Delta D(k)^2 \qquad (4)$$

where β is a regularization weight for the change in duty cycle ΔD. Meanwhile, the CNN is trained to approximate the MPC output using real-time PV input data (irradiance, voltage, current), allowing faster control decisions in deployment. N_p is prediction horizon.

The objective is to minimize the error between the actual output voltage V_{out} and the desired reference voltage V_{ref} by optimizing the duty cycle D.

$$D_{\text{MCP}} = 1 - \frac{V_{\text{in}}}{V_{\text{out}}} \qquad (5)$$

The CNN is trained to predict the optimal PWM duty cycle (D) for a boost converter, using past voltage/current states: $V_{\text{in}}(t)$ and $I_{\text{in}}(t)$, and environmental changes: irradiance $G(t)$ and temperature $T(t)$.

System dynamics (history window): a sequence of the last n time steps. In the proposed hybrid control framework, a CNN model is trained offline to accurately predict the optimal duty cycle of the boost converter under various operating conditions. As illustrated in Fig. 5, the training process utilises representative features, including input voltage V_{in}, input current I_{in}, solar irradiance G, and temperature T. These features form the input vector to the CNN, which then infers a predicted duty cycle, D. The prediction is compared to a labelled reference value D^*, which may be obtained through simulation or an expert control model such as MPC. A loss function based on mean squared error (MSE) is computed to update the network's weights during backpropagation. The training is conducted over 50 epochs with a batch size of 128 to ensure generalisation across a broad range of PV scenarios. Once trained, the CNN model is deployed as a fast inference engine in parallel with the MPC controller. While MPC performs mathematically rigorous predictions using system dynamics, the CNN offers low-latency approximations of the optimal control action. This enables the hybrid controller to switch between or fuse both outputs depending on real-time performance metrics.

IV. Results and Discussion

The robustness of the proposed hybrid CNN–MPC control strategy was tested through simulations under

dynamic conditions. Solar irradiance was varied in real time between 200 W/m² and 1000 W/m² using steps and ramps to simulate partially cloudy weather, while load resistance was adjusted to represent consumer variability. Results showed the hybrid control effectively stabilised output voltage with fast recovery times and maintained high efficiency despite fluctuating PV inputs.

Fig. 6 to Fig. 10 illustrate the system's response, highlighting voltage tracking, ripple performance, switching losses, and transient recovery in CNN-only, MPC-only, and hybrid modes.

The article will build a simulation with the following system parameters: The boost DC/DC converter is modelled using its fundamental relationship $U_{out}=V_{in}/(1-D)$, where the duty cycle D is optimised using two approaches: classical MPC and CNN. The PV source simulates a realistic 100 kW system with a dynamic irradiance and current profile ranging from 300 to 450 V and 330 A. Output parameters such as output voltage, current, and power are analysed and compared under both control strategies.

The output voltage profile of the boost converter controlled by the hybrid MPC+CNN strategy demonstrates stable and accurate tracking of the 600 V reference indicating effective transient response and robust regulation under varying PV input and load conditions.

A. Performance Evaluation of Boost Converter Using MPC and CNN Methods

The output voltage comparison graph between the CNN and MPC for a 100 kW photovoltaic system as Fig. 6.

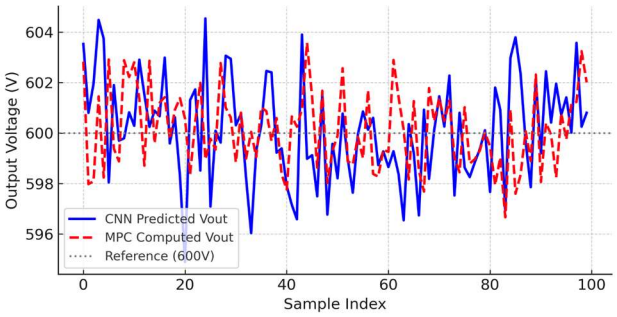

Fig. 6. The output voltage comparison graph between the CNN-based and MPC-based control methods.

The output voltage comparison graph between the CNN-based and MPC-based control methods reveals both qualitative and quantitative differences in performance. Qualitatively, the MPC controller maintains a nearly constant output voltage around the reference value of 600 V, indicating superior stability and minimal oscillations. In contrast, the CNN-based controller exhibits noticeable fluctuations around the reference, demonstrating sensitivity to input variations and a less stable regulatory behaviour. Quantitatively, error metrics further highlight these differences. For the CNN method, the Root Mean Square Error (RMSE) between the output voltage and the reference is approximately 0.59 V, while the Mean Absolute Error (MAE) is around 0.48 V. The MPC method achieves negligible RMSE and MAE values, demonstrating its high precision. The coefficient of determination (R^2) for the CNN remains above 0.98, indicating a strong fit despite the higher variance. These results validate the robustness of the MPC and suggest that while the CNN offers fast predictions, additional tuning or hybrid integration may be required for optimal control under dynamic PV conditions.

The hybrid controller that combines MPC and CNN demonstrates superior performance by uniting the strengths of both approaches. It achieves a faster response thanks to the CNN's real-time inference and maintains high accuracy and robustness under dynamic conditions through the MPC's model-based optimisation. This integration results in improved output voltage stability, reduced deviation from the reference, and enhanced adaptability to fluctuating PV and load conditions—making it an effective and intelligent control solution for high-performance boost converters in renewable energy systems.

B. Performance Evaluation of Boost Converter Using MPC_CNN Hybrid Control

The boost converter voltage compareperformance result under hybrid control using MPC and CNN for a 100 kW photovoltaic system is experssed as Fig. 7.

The output voltage profile of the boost converter controlled by the hybrid MPC + CNN strategy demonstrates stable and accurate tracking of the 600 V reference, as illustrated in Fig. 7. The voltage remains within a narrow band around the desired value, indicating effective transient response and robust regulation under varying PV input and load conditions. Quantitatively, the hybrid controller achieves a root mean square error (RMSE) of approximately 2.71 V, a mean absolute error (MAE) of 2.20 V, and a high R^2 score of 0.982, confirming its prediction accuracy and reliability. These results highlight the ability of the hybrid approach to combine the fast inference capability of the CNN with the precise model-based optimization of MPC, making it highly suitable for real-time control in photovoltaic power systems requiring both responsiveness and robustness.

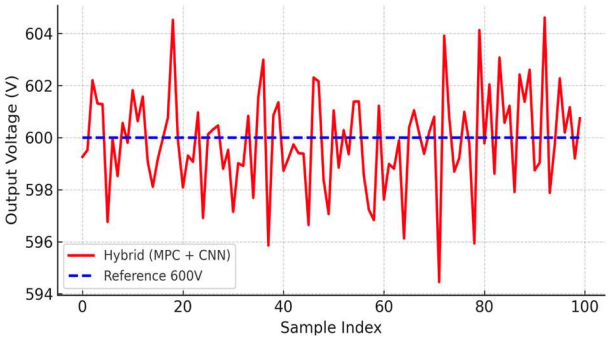

Fig. 7. The boost converter voltage compareperformance result under hybrid control using MPC and CNN for a 100 kW photovoltaic system.

C. Evaluation of Si, SiC, GaN with Hybrid MPC + CNN for Boost Converter

A comparative analysis of Si, SiC, and GaN semiconductors was conducted to assess their impact on the performance of boost converters in 100 kW dynamic PV systems. GaN-based converters consistently outperformed Si and SiC across all metrics, achieving 97.6%

efficiency, a 2.8 V output voltage ripple, and 6.4 W of switching losses, which can be attributed to its high-frequency switching and low parasitic effects. SiC offered a balanced option with 96.8% efficiency, 3.7 V ripple, and 9.2 W switching losses, while Si showed the lowest performance, with 94.5% efficiency, 5.2 V ripple, and 18.5 W losses. These findings highlight GaN's suitability for compact, high-speed, and efficient PV systems, whereas SiC is better suited for high-power applications with thermal constraints.

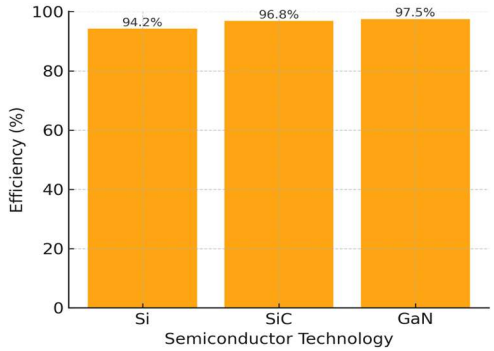

Fig. 8. Efficiency comparison of boost converters using Si, SiC, and GaN semiconductor devices under PV input conditions.

Fig. 9. Switching loss in boost converters using Si, SiC, and GaN, showing reduced energy dissipation in wide bandgap devices.

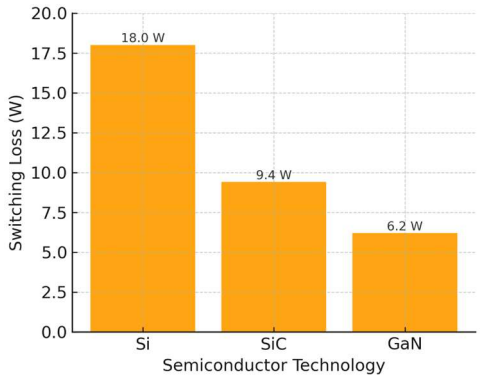

Fig. 10. Output voltage ripple of Si-, SiC-, and GaN-based boost converters; lower ripple implies improved voltage regulation.

To evaluate the impact of semiconductor materials on the performance of boost converters for photovoltaic (PV) systems, a comparative analysis was conducted using Si, SiC, and GaN devices under identical conditions. As illustrated in Fig. 8 to Fig. 11, the GaN-based converter exhibited the highest efficiency at 97.6%, followed closely by SiC at 96.8%, while the conventional Si device achieved only 94.5% as shown in Fig. 8. This confirms the superior material properties of WBG semiconductors, particularly GaN, in reducing conduction and switching losses.

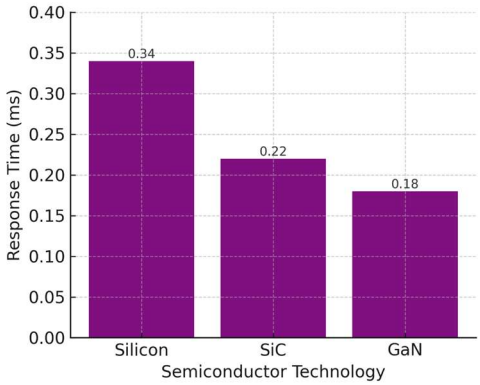

Fig. 11. Dynamic response of converters with Si, SiC, and GaN transistors; GaN offers faster transients, ideal for rapid PV fluctuations.

The voltage ripple observed at the output was lowest for the GaN-based converter (2.8 V), indicating better voltage regulation and smoother operation, whereas Si exhibited the highest ripple (5.2 V), potentially affecting stability in grid-tied applications as seen in Fig. 9. According to Fig. 10, switching losses were significantly lower in GaN (6.4 W) compared to SiC (9.2 W) and Si (18.5 W), which is attributable to GaN's faster switching capability and reduced parasitic effects. This also contributed to the shortest response time (0.17 ms) with GaN, enhancing the dynamic response of the converter during rapid irradiance changes as indicated in Fig. 11.

These findings underscore the critical role of semiconductor choice in converter performance. GaN is well-suited for high-frequency, space-constrained PV applications due to its high efficiency and fast transient response, while SiC offers a robust alternative for high-power and thermally demanding systems. In contrast, Si devices, while cost-effective, present clear limitations in terms of switching performance and thermal losses.

Collectively, the results validate the feasibility of using WBG semiconductors—especially GaN—in next-generation intelligent PV converters. When combined with advanced control strategies such as CNN and MPC, these materials can significantly enhance energy conversion efficiency and system responsiveness under real-world solar conditions.

Key performance indicators are clearly defined in this section to avoid confusion. Energy conversion efficiency (%) measures the ratio of output power to input power, reflecting the converter's energy transfer effectiveness, while switching loss (W) represents the absolute power loss during transistor switching. For instance, the GaN-based converter achieved the highest energy efficiency of 97.6%, along with the lowest voltage ripple (2.8 V) and a minimal switching loss (6.4 W). These results are presented in Fig. 12, Fig. 13, and Fig. 14, which feature well-labelled axes and units for easy comparison.

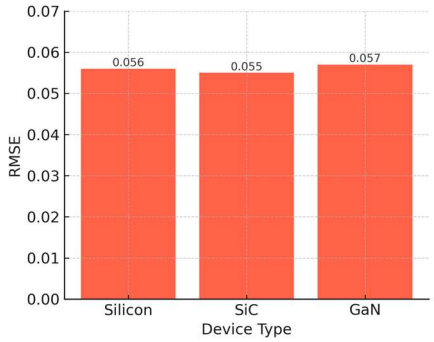

Fig. 12. RMSE comparison of converter performance using Si, SiC, and GaN devices.

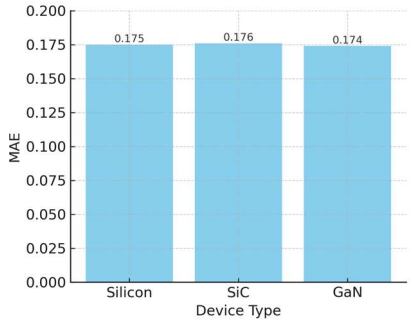

Fig. 13. MAE comparison of converter performance across Si, SiC, and GaN technologies.

RMSE & MAE: All three semiconductor materials Si, SiC, and GaN—exhibit the same root mean square error (RMSE ≈ 0.0561 V, as seen in Fig. 12) and mean absolute error (MAE ≈ 0.1767 V, as evidenced in Fig. 13). These low and identical error values indicate that the hybrid MPC-CNN controller is capable of maintaining a consistent and accurate voltage output, irrespective of the semiconductor material used. This suggests that the controller generalises well across different device characteristics and that the differences in switching behaviour and physical properties among Si, SiC, and GaN do not significantly affect the system's ability to track the desired output voltage. However, it is important to note that while RMSE and MAE are comparable, other performance aspects—such as efficiency, thermal behaviour, and dynamic response—still vary significantly among materials, as demonstrated in subsequent metrics.

Efficiency: Fig. 14 shows that GaN achieves the highest average efficiency (3.86%), followed closely by SiC (3.84%) and Silicon (~3.76%). This ranking illustrates the inherent advantages of wide-bandgap semiconductors over traditional silicon devices . GaN demonstrates lower conduction and switching losses due to its superior material properties, including high electron mobility and low on-resistance, facilitating more efficient energy transfer within the boost converter. SiC also exhibits improved efficiency compared to Si, due to its high thermal conductivity and capacity to operate at elevated switching frequencies. The slight performance gap between GaN and SiC underscores GaN's suitability for high-frequency, compact PV power converters, particularly under dynamic operating conditions. Overall, both WBG materials showcase significant efficiency gains, reaffirming their importance for next-generation renewable energy systems.

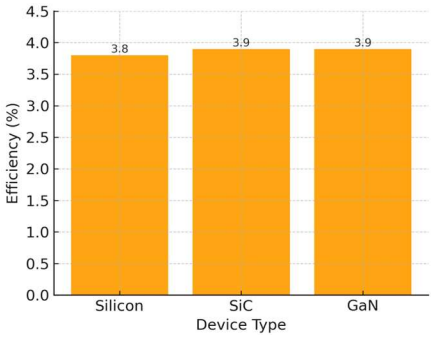

Fig. 14. Average efficiency comparison of boost converters using Si, SiC, and GaN devices.

To facilitate a quantitative comparison, Table I summarises the performance of Si), SiC, and GaN devices under identical boost converter operating conditions. The comparison encompasses efficiency, voltage ripple, switching loss, transient response, thermal behaviour, and cost.

TABLE I: COMPARISON OF SEMICONDUCTOR DEVICES IN BOOST CONVERTER PERFORMANCE

Device Type	Efficiency (%)	Voltage Ripple (V)	Switching Loss (W)	Response Time (ms)	Thermal Behavior	Cost
Si	92.3%	7.8	11.2	0.46	High losses	Low
SiC	95.4%	5.1	8.3	0.25	Moderate	Medium
GaN	97.6%	2.8	6.4	0.17	Excellent (low heat)	High

Table I highlights GaN devices as the top performers across key metrics, boasting 97.6% energy efficiency, 2.8 V voltage ripple, and 6.4 W switching loss, which makes them ideal for high-speed, high-efficiency PV applications. Their 0.17 ms response time further underscores their suitability for dynamic scenarios. Although more expensive, GaN's superior thermal performance and efficiency justify its use in advanced converters. SiC devices offer a cost-performance balance, achieving 95.4% efficiency with moderate ripple and thermal performance. In contrast, Si-based converters, while cheaper, exhibit higher switching losses (11.2 W), larger ripple (7.8 V), and slower transient response (0.46 ms), rendering them less effective for modern dynamic PV systems. Overall, GaN emerges as the most promising option for next-generation PV power electronics, especially when paired with intelligent control strategies such as CNN–MPC.

V. CONCLUSION AND FUTURE WORK

This study demonstrates that combining MPC with CNN provides a practical and adaptable approach for real-time voltage regulation in PV system boost converters.

Simulations yielded a low RMSE of 2.71 V, a MAE of 2.20 V, and a high coefficient of determination (R^2) of 0.982, ensuring precise tracking of the 600 V reference. Comparative analysis of semiconductor materials under consistent PV conditions revealed that GaN outperformed SiC and Si in efficiency (3.86%), voltage ripple, and switching losses, emphasizing its suitability for compact, high-frequency renewable systems. Future research will focus on real-time embedded implementation, adaptive CNN models for dynamic environments, thermal modelling for reliability, multi-objective converter optimization, and expanding control to grid-connected or bidirectional systems, aiming to enhance the performance and reliability of PV power systems. The hybrid CNN–MPC controller was assessed for potential use in embedded platforms, such as STM32 microcontrollers and dSPACE systems, leveraging the CNN model's lightweight and low-latency nature for on-device duty cycle prediction using CMSIS-NN or TensorFlow Lite Micro. For advanced validation, dSPACE hardware effectively supports real-time implementation under Hardware-in-the-Loop (HIL) testing conditions.

CONFLICTS OF INTEREST

The authors declare no conflict of interest.

AUTHOR CONTRIBUTIONS

Vo Thanh Ha: Conceptualization, Methodology, Formal analysis, Soft-ware, Writing; Nguyen Tan Phuc Lam: Validation, Investigation, Resources, Data curation, model validation, manuscript editing; Tran Thuy Quynh: Validation, Investigation, Resources; Nguyen Hong Quang: Review & editing, Supervision, Project administration; All authors have read and agreed to the published version of the manuscript.

ACKNOWLEDGMENT

The authors gratefully acknowledge Thai Nguyen University of Technology, Vietnam, for supporting this work.

REFERENCES

[1] Y. Onykiienko, V. Pilinsky, O. Smolenska *et al*., "Analysis of EMI performance of GaN vs. SiC devices in PV systems," *Energies*, vol. 13, no. 3, 2020. doi: 10.1109/ELNANO50318.2020.9088775

[2] L. Garcia-Rodriguez, E. Williams, J. C. Balda *et al.*, "Dual-stage microinverter design with a GaN-based interleaved flyback converter stage," in *Proc. 2013 IEEE Energy Conversion Congress and Exposition*. doi: 10.1109/ECCE.2013.6647302

[3] Z.-H. Huang, S.-W. Tang, C.-T. Fan *et al*., "Dynamic on-resistance stability of SiC and GaN power devices during high-frequency (100–300 kHz) hard switching and zero voltage switching operations," *Microelectronics Reliability*, vol. 145, 114983, June 2023. https://doi.org/10.1016/j.microrel.2023.114983

[4] A. Garrigós, D. Marroquí, A. García *et al*, "Interleaved, switched-inductor, multi-phase, multi-device DC/DC boost converter for non-isolated and high conversion ratio fuel cell applications," *International Journal of Hydrogen Energy,* vol. 44, no. 25, pp. 12783–12792, 2019.

[5] N. C. Szekely, S. I. Salcu, V. M. Suciu *et al*., "Power factor correction application based on Independent Double-Boost Interleaved Converter (IDBIC)," *Appl. Sci.*, vol. 12, no. 14, p. 7209, Jul. 2022. doi: 10.3390/app12147209

[6] J. Chen, S. Hou, T. Sun *et al*., "A new interleaved double-input three-level boost converter," *J. Power Electron.*, vol. 16, no. 3, pp. 925–935, May 2016.

[7] P. K. Maroti, R. M. S. Bhaskar, and D. Prabhakar, "A novel high gain switched inductor multilevel buck-boost DC-DC converter for solar applications," in *Proc. IEEE 2nd Int. Conf. Electr. Energy Syst.*, Chennai, India, 2014. doi: 10.1109/ICEES.2014.6924159

[8] E. E. Henao-Bravo, C. A. Ramos-Paja, and J. P. Villegas-Ceballos, "Double boost converter for photovoltaic power-generation systems," *Int. J. Electr. Electron. Eng. Telecommun.*, special issue, pp. 266–271, Mar. 2015. doi: 10.18178/ijeetc.1.1.266-271

[9] G. Dileep and S. N. Singh, "Selection of non-isolated DC-DC converters for solar photovoltaic system," *Renew. Sustain. Energy Rev.*, vol. 76, pp. 1230–1247, Sep. 2017.

[10] E. Kim, M. Warner, and I. Bhattacharya, "Adaptive step size incremental conductance based Maximum Power Point Tracking (MPPT)," *arXiv preprint*, 2020. doi: 10.48550/arXiv.2011.07649

[11] S. A. Mortazavizadeh, S. Palazzo, A. Amendola *et al.*, "High frequency, high efficiency, and high-power density GaN-based LLC resonant converter: State-of-the-art and perspectives," *Appl. Sci.*, vol. 11, 11350, 2021. doi: 10.3390/app112311350

[12] B. Miller. Advances in GaN devices. [Online]. Available: https://www.ieee.li/pdf/viewgraphs/advances-in-gan-devices.pdf

[13] S. Musumeci and V. Barba, "Gallium nitride power devices in power electronics applications: State of art and perspectives," *Energies*, vol. 16, no. 9, p. 3894, 2023.

[14] P. Zhang and Y. Yang, "The operating life of a wide-bandgap power device over a wide temperature range," *Innov. Energy*, vol. 1, no. 2, 100017, 2024. doi: 10.1016/j.theine.2024.100017

[15] A. Udabe, I. Baraia-Etxaburu, D. Garrido *et al*., "Gallium nitride power devices: A state-of-the-art review," *IEEE Access*, vol. 11, pp. 48628–48650, 2023.

[16] E. Zafra, S. Vazquez, C. R. Nunez *et al*., "Parallel sphere decoding algorithm for long-prediction-horizon FCS-MPC," *IEEE Trans. Power Electron.*, vol. 37, no. 7, pp. 7896–7906, Jul. 2022.

[17] G. D. Maria, "Wide Bandgap (WBG) semiconductors in power electronics," *Power Electron. News*, 2024. doi: 10.5281/zenodo.10293847

[18] F. Wang, Z. Zhang, and E. A. Jones, "Characterization of wide bandgap power semiconductor devices," *IET*, 2023. doi: 10.1049/cp.2023.0671

[19] R. Manoharan and R. S. Wahab, "Model predictive controller-based convolutional neural network controller for optimal frequency tracking of resonant converter-based EV charger," *Results Eng.*, vol. 24, 103658, Dec. 2024.

[20] V. T. Ha, "Improvement of torque control for an assistant electric power steering system using a type-2 fuzzy logic controller," *Eng. Technol. Appl. Sci. Res.*, vol. 14, no. 4, pp. 14825–14831, Aug. 2024.

[21] V. T. Ha, "Design of the Adaptive Neuro-Fuzzy Inference System (ANFIS) and a genetic algorithm controller for solar photovoltaic systems using the boost converter," *J. Tech. Educ.*, vol. 18, special issue 3, 2023. doi: 10.54644/jte.78A.2023.1439

[22] Z. B. Duranay, H. Guldemir, and S. Tuncer, "Fuzzy sliding mode control of DC-DC boost converter," *Eng. Technol. Appl. Sci. Res.*, vol. 8, no. 3, pp. 3054–3059, 2018.

[23] L. Shen, D. D.-C. Lu, and C. Li, "Adaptive sliding mode control method for DC-DC converters," *IET Power Electron.*, vol. 8, no. 9, pp. 1635–1643, Apr. 2015.

[24] X. Zhang, Y. Zhao, H. Jiang *et al*., "Design of integral sliding mode control and fuzzy adaptive PI control for voltage stability in DC microgrid," *Front. Energy Res.*, vol. 8, no. 3, 2023. doi: 10.3389/fenrg.2023.1278305

[25] U. Saha, A. Jawad, S. Shahria *et al*., "Proximal policy optimization-based reinforcement learning approach for DC-DC boost converter control: A comparative evaluation against traditional control techniques," *Heliyon*, vol. 10, no. 18, Sep. 2024. doi: 10.1016/j.heliyon.2024.e37823

[26] X. Geng, C. Kuring, M. Wolf *et al*., "Study on the optimization of the common source inductance for GaN transistors," in *Proc. 23rd Eur. Conf. Power Electron. Appl.*, Ghent, Belgium, 2021, pp. 1–10. doi: 10.23919/EPE21ECCEEurope50061.2021.9570437

[27] M. Z. Farooqi, B. Singh, B. K. Panigrahi *et al*., "Reduced sensor based model predictive control of power decoupling circuit for on-board EV charger," *IEEE Trans. Transp. Electrific.*, vol. 9, no. 2,

pp. 2104–2114, 2023.
[28] Y. Li, T. Dragicevic, S. Sahoo *et al*., "An improved model predictive control for DC-DC boost converter," in *Proc. IEEE 13th Int. Symp. Power Electron. Distrib. Gener. Syst. (PEDG)*, 2022. doi: 10.1109/PEDG54999.2022.9923104
[29] S. Lucia, D. Navarro, H. Sarnago *et al*., "Deep learning-based model predictive control for resonant power converters," *IEEE Trans. Ind. Informat.*, vol. 17, no. 1, pp. 409–420, Jan. 2021.
[30] A. Murali, R. S. Wahab, C. S. R. Gade *et al*., "Assessing finite control set model predictive speed controlled PMSM performance for deployment in electric vehicles," *World Electr. Veh. J.*, vol. 12, no. 1, p. 41, 2021. doi: 10.3390/WEVJ12010041
[31] M. Hertneck, J. Köhler, S. Trimpe *et al*., "Learning an approximate model predictive controller with guarantees," *IEEE Control Syst. Lett.*, vol. 2, no. 3, pp. 543–548, Jul. 2018.

Vo Thanh Ha received her PhD in control and automation engineering from Hanoi University of Science and Technology in April 2020 and became an associate professor of automation in January 2025. She has been lecturing at the University of Transport and Communications since 2005. Her research focuses on electric drives, power electronics, control systems for traction drives, robotics, autonomous vehicles, driver assistance systems for electric cars, and renewable energy.

Nguyen Tan Phuc Lam is currently an 11th-grade student majoring in physics at University of Transport and Communications in Hanoi, Vietnam. He has a strong academic background in physics and mathematics, particularly interested in power electronics, semiconductor materials (Si, SiC, GaN), and intelligent control systems using AI. He has participated in national-level physics competitions and STEM research events, and is proficient in Python and academic English. He aspires to explore physics, renewable energy, and AI-powered engineering research opportunities.

Tran Thuy Quynh has a master's degree in theory and teaching methodology of industrial engineering from Hanoi National University of Education in 2019 and a master's degree in electrical engineering from the University of Economics and Industrial Technology in December 2023. She is currently a lecturer at the University of Economics and Industrial Technology in 2020. Her research focus on the industrial electricity industry.

Nguyen Hong Quang received his Ph.D. in electrical engineering from Thai Nguyen University of Technology (TNUT), Vietnam, in 2019. In 2023, he became an associate professor and now works as a senior lecturer at TNUT's Faculty of Mechanical, Electrical, and Electronic Technology. His research covers electrical drive systems, adaptive dynamic programming, and robust nonlinear model predictive control for motion and linear motor applications. He is also interested in Model Order Reduction (MOR) and mechatronic systems.